

ON THE ENERGY OF <100> COINCIDENCE TWIST BOUNDARIES
IN
TRANSITION METAL OXIDES

by

Dieter Wolf

MASTER

DISCLAIMER

This book was prepared as an account of work sponsored by an agency of the United States Government. Neither the United States Government nor any agency thereof, nor any of their employees, makes any warranty, express or implied, or assumes any legal liability or responsibility for the accuracy, completeness, or usefulness of any information, apparatus, product, or process described, or represents that its use would not infringe privately owned rights. Reference herein to any specific commercial product, process, or service by trade name, trademark, manufacturer, or otherwise, does not necessarily constitute or imply its endorsement, recommendation, or favoring by the United States Government or any agency thereof. The views and opinions of authors expressed herein do not necessarily state or reflect those of the United States Government or any agency thereof.

Prepared for
3rd Europhysical Topical Conference
on
Lattice Defects in Ionic Crystals
Canterbury, England
September 17-21, 1979



U of C-AUA-USDOE

DISTRIBUTION OF THIS DOCUMENT IS UNLIMITED

ARGONNE NATIONAL LABORATORY, ARGONNE, ILLINOIS

Operated under Contract W-31-109-Eng-38 for the
U. S. DEPARTMENT OF ENERGY

DISCLAIMER

This report was prepared as an account of work sponsored by an agency of the United States Government. Neither the United States Government nor any agency Thereof, nor any of their employees, makes any warranty, express or implied, or assumes any legal liability or responsibility for the accuracy, completeness, or usefulness of any information, apparatus, product, or process disclosed, or represents that its use would not infringe privately owned rights. Reference herein to any specific commercial product, process, or service by trade name, trademark, manufacturer, or otherwise does not necessarily constitute or imply its endorsement, recommendation, or favoring by the United States Government or any agency thereof. The views and opinions of authors expressed herein do not necessarily state or reflect those of the United States Government or any agency thereof.

DISCLAIMER

Portions of this document may be illegible in electronic image products. Images are produced from the best available original document.

The facilities of Argonne National Laboratory are owned by the United States Government. Under the terms of a contract (W-31-109-Eng-38) among the U. S. Department of Energy, Argonne Universities Association and The University of Chicago, the University employs the staff and operates the Laboratory in accordance with policies and programs formulated, approved and reviewed by the Association.

MEMBERS OF ARGONNE UNIVERSITIES ASSOCIATION

The University of Arizona	The University of Kansas	The Ohio State University
Carnegie-Mellon University	Kansas State University	Ohio University
Case Western Reserve University	Loyola University of Chicago	The Pennsylvania State University
The University of Chicago	Marquette University	Purdue University
University of Cincinnati	The University of Michigan	Saint Louis University
Illinois Institute of Technology	Michigan State University	Southern Illinois University
University of Illinois	University of Minnesota	The University of Texas at Austin
Indiana University	University of Missouri	Washington University
The University of Iowa	Northwestern University	Wayne State University
Iowa State University	University of Notre Dame	The University of Wisconsin-Madison

NOTICE

This report was prepared as an account of work sponsored by an agency of the United States Government. Neither the United States nor any agency thereof, nor any of their employees, makes any warranty, expressed or implied, or assumes any legal liability or responsibility for any third party's use or the results of such use of any information, apparatus, product or process disclosed in this report, or represents that its use by such third party would not infringe privately owned rights. Mention of commercial products, their manufacturers, or their suppliers in this publication does not imply or connote approval or disapproval of the product by Argonne National Laboratory or the United States Government.

On the Energy of $\langle 100 \rangle$ Coincidence Twist Boundaries in
Transition Metal Oxides

D. Wolf
Materials Science Division
Argonne National Laboratory
Argonne, IL 60439

Abstract

The energies of coincidence twist boundaries formed by rotation about a $\langle 100 \rangle$ axis in stoichiometric transition metal oxides crystallizing in the NaCl structure (such as NiO, MnO, and CoO) have been calculated using the ionic-type potentials of Catlow et al. for these materials. From a relaxation calculation it is found that the energies of the most prominent coincidence twist boundaries at 36.87, 22.62, 28.07, and 16.26^o (which correspond to inverse coincidence-site densities of $\Sigma=5, 13, 17,$ and 25, respectively) lie above the energy of the free [100] surface. The reason arises from the repulsive Coulomb interactions between ions in configurations close to "anti-coincidence" (anion on anion or cation on cation) which are capable of overcoming the attractive Coulomb interactions between the ions in coincidence configurations (cation on anion and vice versa). It is concluded that in contrast to metals the structures of $\langle 100 \rangle$ twist boundaries in oxides and alkali halides may not simply be derived from the coincidence lattice geometry. Entropy terms are not considered.

I. Introduction

Recent experimental evidence in support of the existence of high-angle coincidence twist boundaries in metal oxides¹ apparently similar in nature to their metallic counterparts² has greatly stimulated the interest in grain-boundary properties in oxides. Chaudhari and Charbneau³ had predicted the existence of such boundaries for MgO on the basis of simple energy calculations. In contrast to metals, however, their energies were found not to scale with the density Σ^{-1} of coincidence sites.

The unrelaxed structure, for example, of $\langle 100 \rangle$ coincidence twist boundaries on $[100]$ planes not only shows the usual coincidences (in which an anion is positioned directly above a cation or vice versa) but also a number of "almost anti-coincidences" (in which anions or cations rest on top of each other; see Fig. 1). The subsequent existence of both attractive and repulsive long-range Coulomb interactions between ions on opposite sides of the grain boundary suggests that ionic relaxation may play an important role in stabilizing such boundaries. For that reason, in this article relaxation has been taken into account in determining the properties of $\langle 100 \rangle$ coincidence twist boundaries in metal oxides with the NaCl structure. Since reliable interionic potentials are available⁴, as our first example we have chosen NiO for our calculations.

II. Method of Calculation

A. Grain Boundary Unit Cell

The unit cell of the planar superlattice obtained by rotation of two $[100]$ faces of NaCl-type crystals by 36.87° with respect to each other is shown in Fig. 1. x_1, y_1 and x_2, y_2 are the Cartesian coordinate systems associated with the surfaces of two semi-infinite crystals 1 and 2 whose $[100]$ faces have been brought in contact. x_s and y_s denote the coordinate axes of the superlattice thus obtained for an inverse coincidence-

site density of $\Sigma=5$. Other boundaries examined are those for $\Sigma=13$, 17, and 25 corresponding to rotation angles of 22.62° , 23.07° , and 16.26° ; respectively.

A view parallel to the boundary [100] plane P (dashed line) is shown in Fig. 2. To later allow for relaxation of the ionic positions a variable number, n , of lattice planes between the two perfect crystals 1 and 2 is inserted. In Fig. 2, for example, $n=4$. A starting configuration for our calculations is obtained by choosing an initial separation d of the planes on the opposite sides of P. Note that the z axis is a four-fold rotation axis which substantially reduces the number of ions for which detailed calculations have to be performed.

B. Interionic Potential

The interionic potential of Catlow et al.⁴ includes long-range Coulomb, and short-range Born-Mayer and dipole-dipole Van-der-Waals contributions. For simplicity, terms arising from the polarizability of the ions which have been included in Catlow et al.'s potential via the simple shell model have been dropped in our calculations. This simplification reduces the calculated cohesive energy per ion from $U_0 = 41.01$ eV to 40.94 eV. In spite of their simplicity these simple potentials were found to reproduce the ideal-lattice and defect properties of NiO, MnO, CoO, and FeO rather well.⁴

C. Energy Calculation

While the calculation of the short-range interaction energy of a given ion is trivial, the summation over the long-range Coulomb interaction potential is rather involved. The Coulomb energy of an ion in the unit cell may be decomposed as follows (see Fig. 2):

$$U_j^{\text{Coul}} = U_{j-1} + U_{j-2} + \sum_m \frac{q_j q_m}{|\vec{r}_j - \vec{r}_m|}, \quad (1)$$

where $U_{j-\beta}$ denotes the interaction energy of ion j with the semi-infinite crystal β ($\beta=1,2$). The third contribution to U_j^{Coul} represents the interaction energy of j with all other ions in the boundary layer in which relaxation is considered. q_j is the ionic charge of ion j while $\vec{r}_j - \vec{r}_m$ denotes an interionic vector.

According to Lennard-Jones and Dent⁵, for the interaction of j with a [100]-faced semicrystal

$$U_{j-1}(x,y,z) = \frac{4q_1 q_2}{d_o} \sum_{\ell, m = \pm 1, \pm 3, \dots}^{\infty} \sum_{\ell, m = \pm 1, \pm 3, \dots}^{\infty} (-1)^{(\ell+m)/2} \frac{\exp(-2\pi z \sqrt{\ell^2 + m^2} / d_o)}{\sqrt{\ell^2 + m^2} (1 + \exp(-\pi \sqrt{\ell^2 + m^2}))} \cos\left(\frac{\ell x}{d_o} + \frac{m y}{d_o} - \frac{\ell+m}{4}\right), \quad (2)$$

where x, y, z are the coordinates of ion j (in the unit cell) with respect to the surface of crystal 1 with an ion of charge q_1 at the origin.

As seen from Fig. 2, $q_2 = -q_1$; hence

$$U_{j-2}(x,y,z) = -U_{j-1}(x,y,z_0 - z), \quad (3)$$

where z_0 denotes the distance between crystals 1 and 2.

The self energy of ion j in a thin plate of finite thickness was determined by means of a modification of Ewald's three-dimensional method for the limit in which the unit cell is periodically extended in x and y only but not in z . Following Tosi's⁶ terminology and description of that method one can show that for a thin plate of finite thickness

$$\sum_m \frac{q_j - q_m}{\vec{r}_j - \vec{r}_m} = \frac{4\pi q_j}{A} \sum_{\vec{k}_\ell} e^{-\vec{k}_\ell^2 / 4\alpha^2} \sum_n q_n e^{-\vec{k}_\ell \cdot (\vec{r}_n - \vec{r}_j)} - \frac{2\alpha q_j^2}{\sqrt{\pi}} +$$

$$+ q_j \sum_\ell \sum_n q_n \frac{1 - F(|\vec{r}_j - \vec{r}_n - \vec{r}_\ell|)}{|\vec{r}_j - \vec{r}_n - \vec{r}_\ell|}, \quad (4)$$

where $A=a^2$ (see Fig. 1) is the area of the unit cell in the x-y plane. For <100> twist boundaries $a/d_n = \sqrt{2}/2$. \vec{k}_ℓ represents the set of two-dimensional reciprocal lattice vectors associated with the unit cell and its periodic extensions which are characterized by the vectors \vec{r}_ℓ . Finally, the summation over n involves all ions in the unit cell while α denotes a parameter associated with the width of a two-dimensional Gaussian charge distribution. It is to be chosen such that the sums in Eq. (4) converge.

D. Method of Relaxation

Starting from Eqs. (2)-(4) and the appropriate short-range potentials,⁴ the energy, forces, and second derivatives may be calculated for every ion by the method described above. The total energy $U_j(\vec{r}_j)$ may be developed about its unrelaxed position \vec{r}_j^0 as follows:

$$U_j(\vec{r}_j) = U_j(\vec{r}_j^0) - \vec{F}_j(\vec{r}_j^0) \cdot (\vec{r}_j - \vec{r}_j^0) + \frac{1}{2} (\vec{r}_j - \vec{r}_j^0) \cdot \underline{W}_j(\vec{r}_j^0) \cdot (\vec{r}_j - \vec{r}_j^0), \quad (5)$$

where \vec{F}_j denotes the force on ion j while \underline{W}_j is the symmetrical second-rank tensor of the second derivatives at the site of ion j. At equilibrium, $dU_j(\vec{r}_j)/d\vec{r}_j = 0$. Therefore,

$$\vec{r}_j = \vec{r}_j^0 + \underline{W}_j^{-1}(\vec{r}_j^0) \cdot \vec{F}_j(\vec{r}_j^0) \quad (6)$$

may be used as the basis for the iterative minimization of the energy.

of the ions in the grain boundary. $\underline{W}_j^{-1}(\vec{r}_j^0)$ determines the amount by which ion j is to be displaced in the direction of its force components in order to reduce its energy and force. This relaxation method involving the second derivatives has the advantage of faster convergence over the simpler and more widely used gradient method in which the proportionality factor by which the ions are displaced in the direction of their forces is the same for all ions in a given relaxation step.

III. Results

The energy of a twist boundary may be defined as

$$U_{gb} = \sum_j (U_j - U_0)/A \quad , \quad (7)$$

(unit
cell)

where U_0 is the cohesive energy per ion in the ideal crystal (see Sec. IIB).

A. Surface Energy

To test the relaxation procedure described above, U_{gb} was calculated for a hypothetical $\Sigma=1$ boundary which one obtains for $\theta=0$. The energies thus obtained as a function of d (see Fig. 2) are shown in Fig. 3. For $d \gg d_0$, U_{gb} converges towards the surface energy σ . For the unrelaxed surface we found $\sigma=428 \text{ erg/cm}^2$ while after relaxation we obtained $\sigma \approx 375 \text{ erg/cm}^2$. These results were obtained by considering the relaxation of the six lattice planes closest to the [100] surface. A larger number of layers did not change the results. It was found that the cations in the surface layer relax by about 1% of d_0 into the surface while the anions relax by a similar amount out of the surface. Both cations and anions on the second layer were observed to relax towards the free surface. The relaxation was found to extend as far as the fourth layer below the surface. The magnitude of the surface and relaxation energies as well as the characteristics and magnitude of the ionic relaxation are in

general agreement with Tasker's surface energy calculations for many alkali halides.⁷

B. Grain-Boundary Energies

For all four coincidence orientations considered grain-boundary energies larger than the free-surface energy σ were obtained. They are shown as functions of d in Fig. 3. In spite of different partially relaxed starting configurations chosen, it was found impossible to reduce U_{gb} to values below the surface energy. In fact, for $d > d_0$ it was not even possible to reduce U_{gb} below its value for the unrelaxed configuration sketched in Fig. 2. However, by increasing d a lower-energy configuration was obtained in all cases. Note that the values of U_{gb} in Fig. 3 scale with Σ .

IV. Discussion

The physical reason for the instability of the $\langle 100 \rangle$ coincidence twist boundaries considered is closely related to the nature of the Coulomb interaction. With the exception of the ions at the coincidence sites, many ions change their total Coulomb interaction with the crystal on the other side of the boundary from being attractive (for $\theta=0$) to being repulsive (for finite values of θ). For example, the unit cell for $\Sigma=5$ (see Fig. 1) contains eight pairs of ions in "almost anti-coincidence" configurations but only two pairs of ions in coincidence configurations. The situation is even less favorable for larger Σ values; hence the even larger energies in Fig. 3.

In spite of the recent observation¹ of the $\Sigma=5$ and $\Sigma=13$ boundaries in MgO, the following observations strongly support the validity of the results presented:

1. For all values of Σ , U_{gb} converges towards the same surface energy σ which was determined independently.

2. The surface energy and structure as well as the magnitude of the surface relaxation agree rather well with the general findings for the alkali halides.⁷
3. The unrelaxed energies and forces for the ions at the grain boundaries do not depend on the number of lattice planes chosen in which the ions may relax. This suggests that the Coulomb-energy calculation according to Eqs. (1)-(4) is correct.

This leads us to conclude that the structures of $\langle 100 \rangle$ coincidence twist boundaries in oxides and alkali halides cannot simply be derived from the coincidence geometry. This is also suggested by some of the difficulties with which these boundaries have finally been manufactured. Instead, the structure of these boundaries may involve (1) large displacements of ions from the coincidence geometry of the unit cell, (2) point defects in the grain boundary, or (3) serrated non-planar boundary planes on an atomic scale. [Unfortunately a comparison of our results with those of Chaudhari and Charbnaou³ is not possible since for some incomprehensible reason their cohesive energies per ion are lower in the crystal with the grain boundary than in a single crystal. This makes the validity of these results rather dubious. In our opinion their error arises from the improper calculation of the Coulomb energy. Although their free-surface energy calculation appears to be correct, their expression for the interaction energy of an ion above a [100] surface with the semi-infinite rigid single crystal below does not agree with that of Lennard-Jones and Dent⁵ (see Eq. (2)).

Acknowledgements

I am grateful to N. L. Peterson and M. Rühle for stimulating my interest in grain-boundary problems. I have greatly benefited from discussions with R. Benedek on all aspects of this work and with A. Rahman on the application of Ewald's method.

References

1. C. P. Sun and R. W. Balluffi, Scripta Met. (to be published).
2. T. Schober and R. W. Balluffi, Phil. Mag. 21 (1970) 109 and ibid. 24 (1971) 165.
3. P. Chaudhari and H. Charbnau, Surface Science 31 (1972) 104.
4. C. R. A. Catlow, W. C. Mackrodt, M. J. Norgett, and A. M. Stoneham, Phil. Mag. 35 (1977), 177 and ibid. (to be published).
5. J. E. Lennard-Jones and B. M. Dent, Trans. Faraday Soc. 24 (1928) 92.
6. M. P. Tosi, Sol. St. Phys. 16, (1964) 1.
7. P. W. Tasker, Phil. Mag. 39 (1979) 119.

Figure Captions

- Fig. 1. Superlattice formed by rotation of two [100] surfaces of NaCl-type crystals by $\theta=36.87$ degrees about the $\langle 100 \rangle$ axis. The central square shows the ion distribution in the unit cell of the superlattice of this $\Sigma=5$ boundary.
- Fig. 2. Separation of the rigid ideal semi-infinite crystals 1 and 2 by a variable number of lattice planes in which the ions may relax. The ion arrangement sketched is that for the $\Sigma=5$ boundary the structure of which in the x-y plane is shown in Fig. 1. P indicates the boundary plane.
- Fig. 3. Grain-boundary energies as function of the separation d of nearest-neighboring layers at the boundary plane. The values for $\Sigma=13$ (which were omitted from the figure for clarity) lie between those for $\Sigma=5$ and $\Sigma=17$.

$\Sigma = 5; \langle 100 \rangle; \theta = 36.87^\circ$

- O^{2-} IN CRYSTAL 2
- Me^{2+} IN CRYSTAL 2
- Me^{2+} IN CRYSTAL 1
- O^{2-} IN CRYSTAL 1

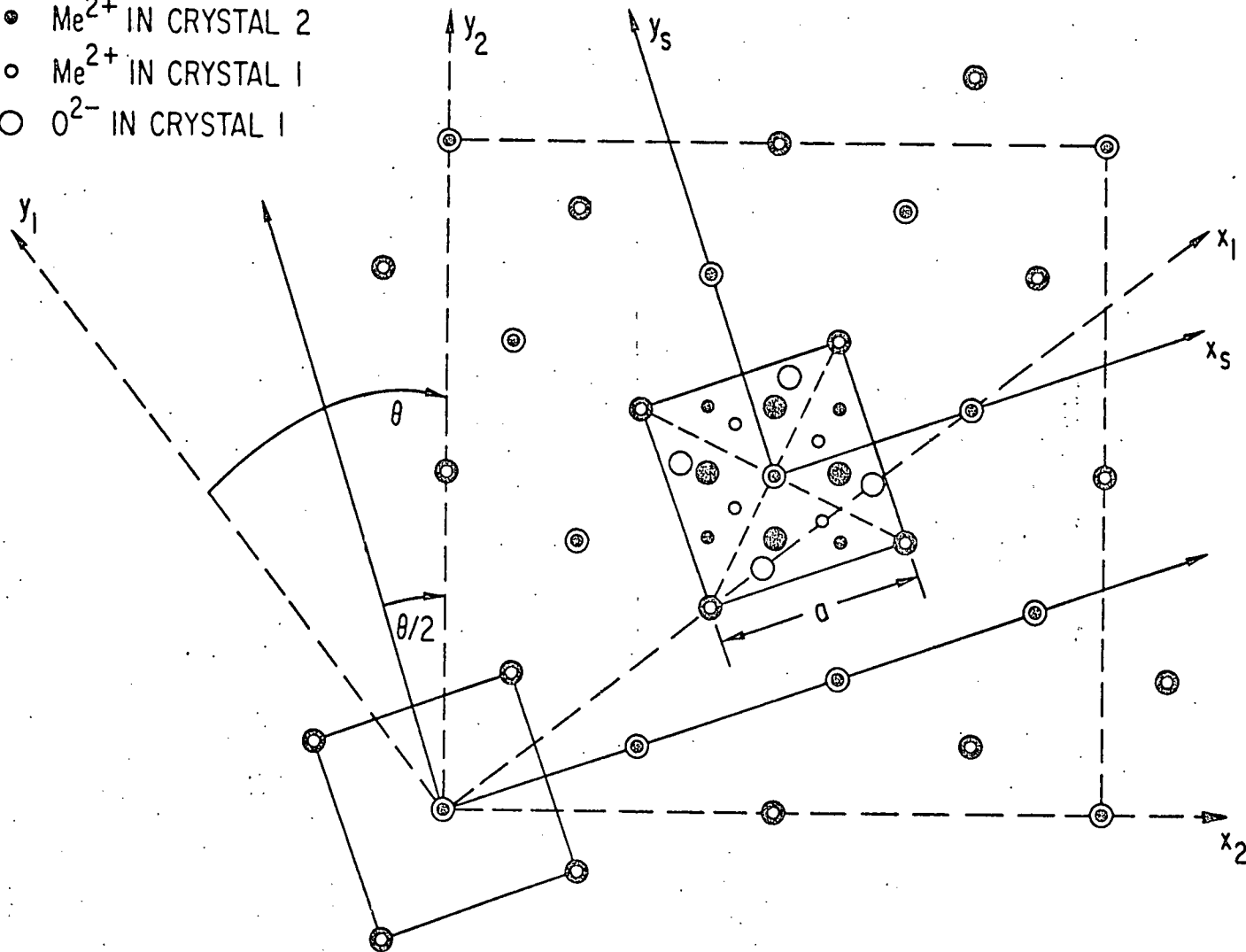


Figure 1.

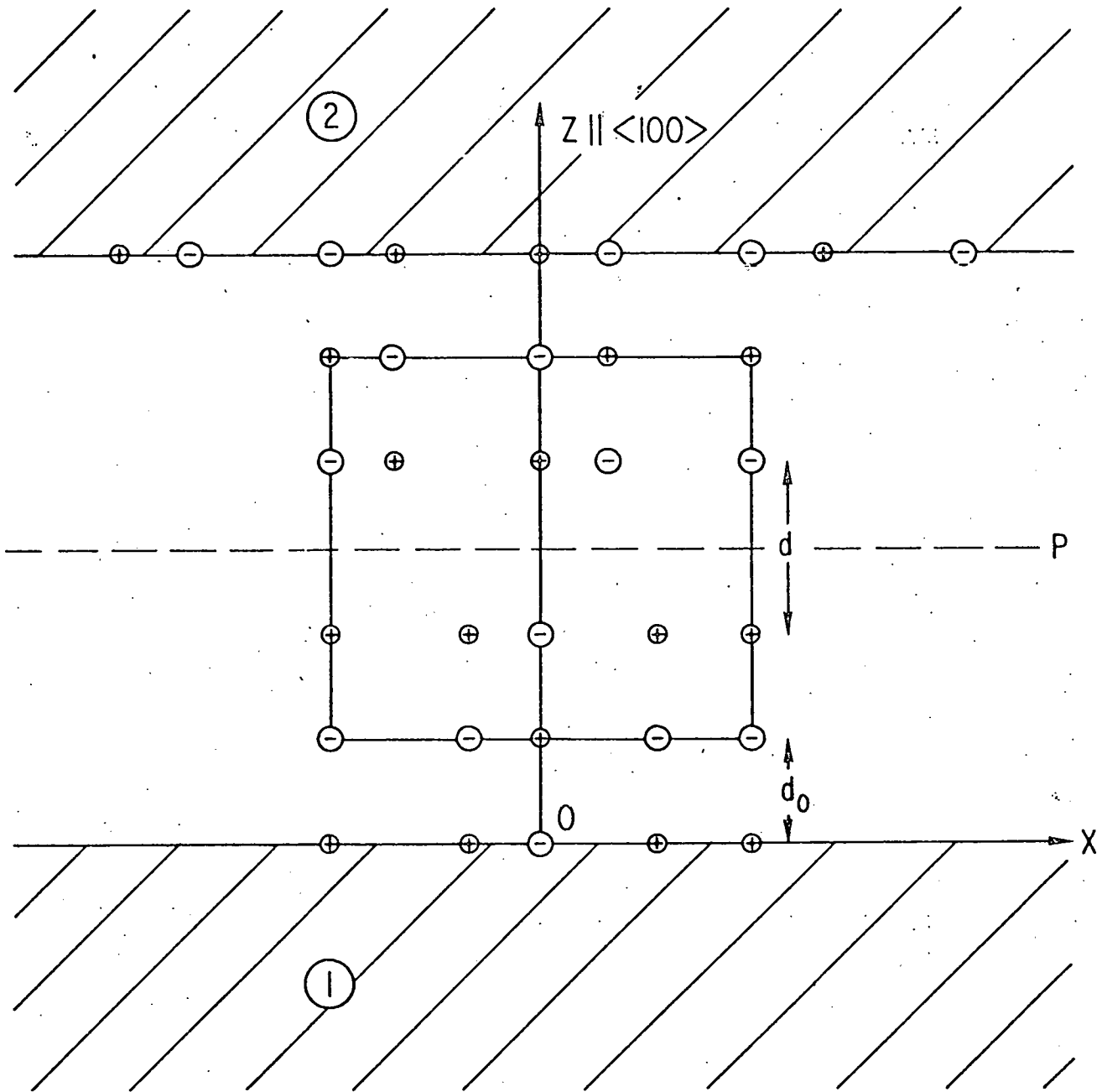


Figure 2.

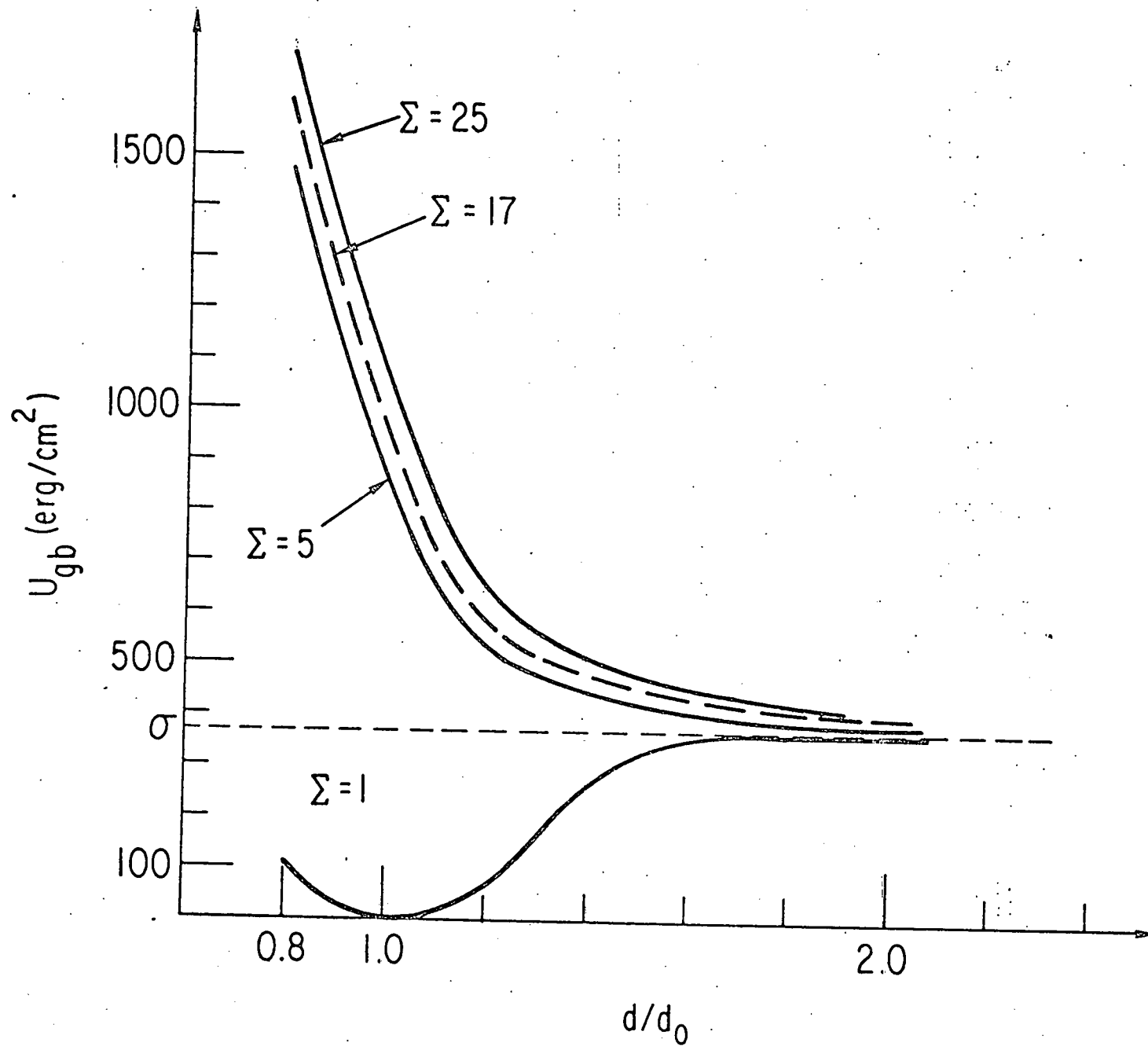


Figure 3.